Helical Polyisocyanides with Fan-Shaped Pendants

Takashi Kajitani,*[†,§] Hongzhen Lin,[‡] Kanji Nagai,[†,‡] Kento Okoshi,[†] Hisanari Onouchi,[†] and Eiji Yashima*[†,‡]

Yashima Super-structured Helix Project, Exploratory Research for Advanced Technology (ERATO), Japan Science and Technology Agency (JST), Japan, and Department of Molecular Design and Engineering, Graduate School of Engineering, Nagoya University, Nagoya, 464-8603, Japan

Received October 17, 2008
Revised Manuscript Received November 20, 2008

Introduction

Optically active polymers with a single-handed helical conformation,[1] exhibiting interesting functions, such as liquid crystals, enantioselective recognition, and catalysts, have drawn considerable attention in the fields of chiral materials science. To this end, optically active helical polymers have been prepared by the polymerization of nonracemic monomers and by the helix-sense selective polymerization of achiral or prochiral monomers with chiral catalysts or initiators.[1,2]

In general, strong attractive or repulsive interactions, such as intramolecular hydrogen bonds[3] and steric hindrance[2a−e,h] between the neighboring pendant groups, respectively, are required for producing optically active helical polymers with a preferred-handed helix sense. However, Veciana and coworkers reported that helical polyisocyanides with an excess left- or right-handed helical conformation could be formed during the polymerization of isocyanides with a stereogenic center positioned far from the polymer backbone. This long-range effect of chirality transfer from the side chains to the polymer backbones was ascribed to the steric effect between the neighboring phenyl benzoates at the pendants.[4] The helicity induction process showed odd−even effects[4a−c,e,5] with respect to the position of the chiral substituent. In addition, the helical polyacetylenes bearing dendritic and fan-shaped pendants with multiple (*S*)-3,7-dimethyloctyloxy chains were prepared by Meijer et al.[6] and Percec et al.,[7] respectively, and the steric effects on their helical conformations were extensively investigated. These helical polyacetylenes formed liquid crystalline (LC) macrostructures in the thermotropic system.[6,7]

Recently, we reported an unprecedented helix-sense-controlled polymerization of enantiomerically pure phenyl isocyanides bearing an L- or D-alanine pendant with a long *n*-decyl chain.[8] In sharp contrast with amino acid- or peptide-bound helical poly(isocyanopeptide)s,[1e,3a,b,d,f] the polymerization with an achiral nickel catalyst ($NiCl_2$) diastereoselectively proceeded, resulting in either a right- or a left-handed helical poly(phenyl isocyanide) whose helix-sense could be controlled by the polymerization solvent and temperature.[8] An intermolecular hydrogen bond between the pendant amide residues of the growing chain end and the monomer during the propagation reaction appeared to play a crucial role in the poly(phenyl isocyanide) either kinetically or thermodynamically forming a stable right- or left-handed helical structure. This speculation was supported by the fact that a poly(phenyl isocyanide) having L-lactic acid residues with the same *n*-decyl chain as that of the pendants exhibited a very weak Cotton effect independent of the polymerization conditions.[9]

In this study, we synthesized a series of novel optically active phenyl isocyanides bearing mono-, di-, or tri-(*S*)-alkoxy chains with stereogenic centers at a different position than that of the pendants (**1a**−**3a** and **1b**−**3b**), and they were polymerized with an achiral $NiCl_2$ or the μ-ethynediyl palladium−platinum (Pd−Pt) complex,[10] which is known to be an effective catalyst for the living polymerization of phenyl isocyanides. The resulting poly(phenyl isocyanide)s (poly-**1a**−poly-**3a**, poly-**1b**−poly-**3b**, poly-**3a′**, and poly-**3b′**) (Chart 1) possess optically active alkoxy chains, and a preferred-handed helix formation cannot be expected through attractive interactions such as hydrogen bonds. We then investigated the steric effects and the position of the stereogenic center (odd−even effect) of the pendant groups of the polymers on their chiroptical and LC properties and helical structures by using circular dichroism (CD) and absorption spectroscopy, polarized optical microscopic (POM) observations, and X-ray diffraction (XRD) measurements.[11]

Experimental Section

Instruments. NMR spectra were measured on a Varian AS500 spectrometer operating at 500 MHz for ^1H and 125 MHz for ^{13}C or a Varian Mercury-300 spectrometer operating at 300 MHz for ^1H and 75 MHz for ^{13}C, respectively, using TMS as an internal standard. IR spectra were recorded using a JASCO FT/IR-680 spectrophotometer. The absorption and CD spectra were obtained in a 1.0 mm quartz cell using a JASCO V570 spectrophotometer and a JASCO J820 spectropolarimeter, respectively. The temperature was controlled with JASCO ETC-505 and CDF-426 apparatuses for absorption and CD measurements, respectively. The polymer concentration was calculated on the basis of the monomer units and was 0.2 mg/mL. Size exclusion chromatography (SEC) was performed using a JASCO PU-2080 liquid chromatograph equipped with UV−visible (JASCO UV-2070) and RI (JASCO RI-2031) detectors. Two Tosoh TSKgel Multipore H_{XL}-M GPC columns (30 cm) were connected in series, and THF containing 0.1 wt % tetra-*n*-butylammonium bromide (TBAB) was used as the eluent at a flow rate of 1.0 mL/min. The molecular weight calibration curve was obtained with standard polystyrenes (Tosoh). POM observations were carried out with an E600POL polarizing optical microscope (Nikon) equipped with a DS-5M CCD camera (Nikon) connected with a DS-L1 control unit (Nikon). The wide-angle X-ray diffraction (WAXD) and small-angle X-ray scattering (SAXS) measurements were carried out using a Rigaku RINT RAPID-R X-ray diffractometer (Rigaku, Tokyo, Japan) with a rotating anode generator and graphite-monochromated CuKα radiation (0.15418 nm) focused through a 0.3 mm pinhole collimator, which was supplied at a 45 kV voltage and a 60 mA current, equipped with a flat imaging plate with specimen-to-plate having distances of 120.0 and 699.5 mm from the sample position, respectively. The SAXS measurements were performed at 200 °C, and the WAXD measurements were performed at 200 °C or ambient temperature.

Materials. Anhydrous tetrahydrofuran (THF), dichloromethane (CH_2Cl_2), chloroform ($CHCl_3$), ethyl acetate, ethanol, and methanol (water content <50 ppm) were purchased from Wako (Osaka, Japan). Nickel(II) chloride hexahydrate ($NiCl_2 \cdot 6H_2O$), (*S*)-(+)-citronellyl bromide (purity >95%), and (*S*)-(+)-1-bromo-2-methylbutane (purity >99%) were obtained from Aldrich. Formic acid, acetic anhydride, triphosgene, and triethylamine were purchased from Wako, Tokyo Kasei (TCI, Tokyo, Japan), or Aldrich. These

---

* Corresponding authors. E-mail: kajitani@riken.jp; yashima@apchem.nagoya-u.ac.jp.

[†] Japan Science and Technology Agency (JST).

[‡] Nagoya University.

[§] Present address: Advanced Science Institute, RIKEN, 2-1 Hirosawa, Wako, Saitama 351-0198, Japan.

10.1021/ma802345g CCC: $40.75

Chart 1. Structures of Polyisocyanides

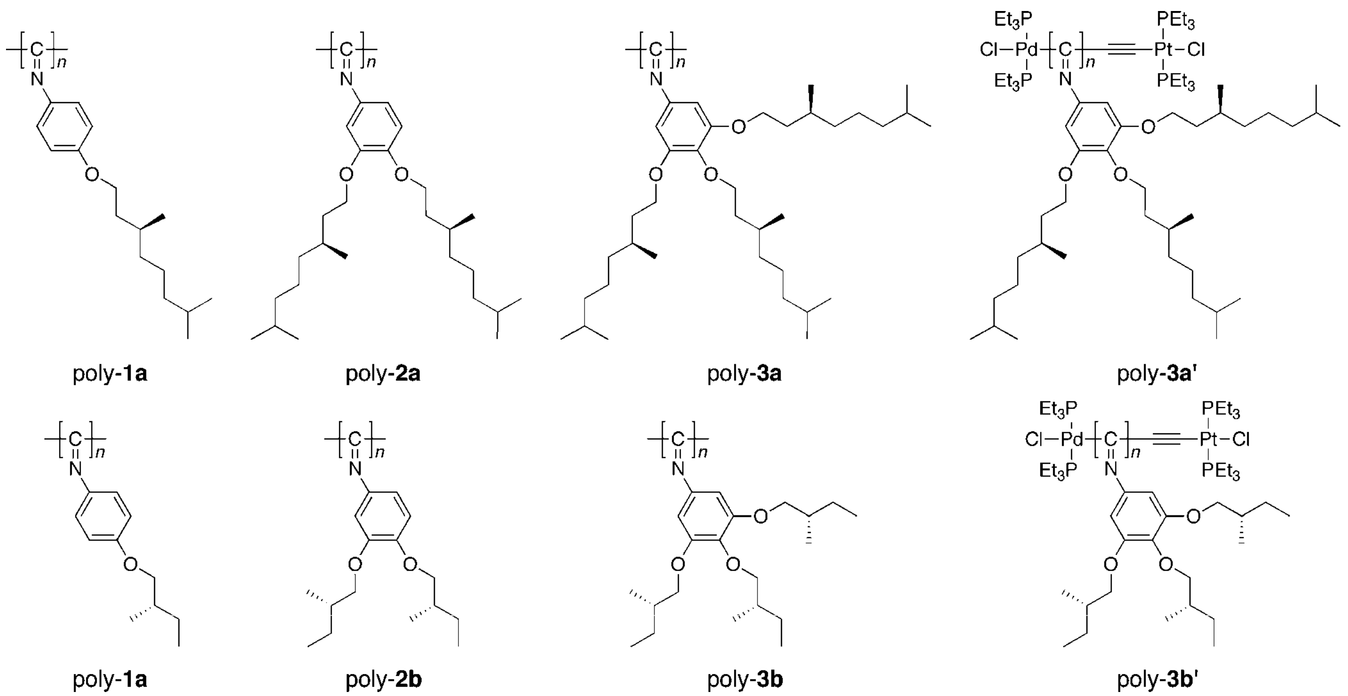

Scheme 1. Synthesis and Polymerization of Phenyl Isocyanides (1–3) with $NiCl_2 \cdot 6H_2O$

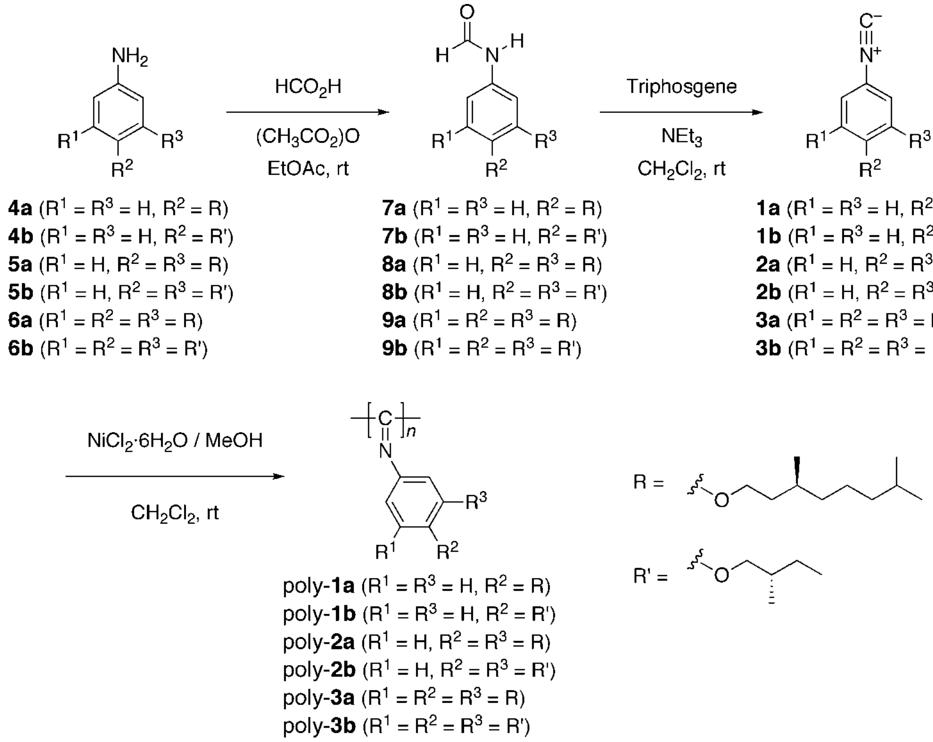

reagents were used without further purification. The μ-ethynediyl palladium–platinum (Pd–Pt) complex[10a] and mono-, di-, and trialkoxyanilines (**4**–**6**)[12] were prepared as previously reported. Polyisocyanides (poly-**1**–poly-**3**) were prepared according to Schemes 1[8] and 2.[10b,13]

Typical Procedure for Syntheses of 7–9. After a mixture of formic acid (1.02 mL, 27.1 mmol) and acetic anhydride (0.511 mL, 5.41 mmol) was stirred at room temperature for 1 h under Ar, 4-((*S*)-3,7-dimethyloctyloxy)aniline (**4a**) (1.35 g, 5.41 mmol) in dry ethyl acetate (10 mL) was added to the mixture at 0 °C. The dispersion solution was stirred at 0 °C for 30 min and then at room temperature for 30 min. To the solution was added ethyl acetate (50 mL), and the mixture was filtered. The filtrate was washed with H_2O (100 mL) and then dried over anhydrous $MgSO_4$. After the solvent was removed under reduced pressure, the crude product was purified by SEC with $CHCl_3$ as the eluent to produce **7a** as a brown oil (0.93 g, 62%). IR (neat, cm^{-1}): 3278 (ν_{N-H}), 1676 (amide I), 1542 (amide II), 1245 (ν_{C-O} ether). ^1H NMR ($CDCl_3$, rt, 500 MHz, δ): 0.87 (d, J = 7.0 Hz, CH_3, 6H), 0.94 (d, J = 7.0 Hz, CH_3, 3H), 1.10–1.38 (m, CH_2, 6H), 1.47–1.62 (m, CH_2, 2H), 1.64–1.72 (m, CH, 1H), 1.78–1.87 (m, CH, 1H), 3.93–4.04 (m, CH_2, 2H), 6.87 (d, J = 8.5 Hz, H_m to NH in trans, 0.7H), 6.90 (d, J = 8.5 Hz, H_m to NH in cis, 1.3H), 7.04 (d, J = 8.5 Hz, H_o to NH in cis, 1.3H), 7.44 (d, J = 8.5 Hz, H_o to NH in trans, 0.7H), 8.12 (s, HCO in cis,

Scheme 2. Polymerization of Phenyl Isocyanides (3a and 3b) with *μ*-Ethynediyl Pd−Pt Complex

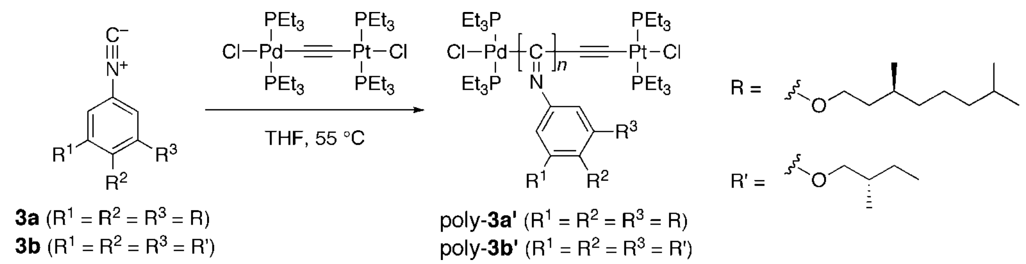

0.4H), 8.25 (s, NH in cis, 0.4H), 8.31 (s, HCO in trans, 0.6H), 8.50 (d, J = 11.0 Hz, NH in trans, 0.6H). ^{13}C NMR ($CDCl_3$, rt, 125 MHz, δ): 19.87, 22.82, 22.92, 24.87, 28.19, 30.06, 36.36, 37.49, 39.45, 66.85, 115.73, 121.92, 126.56, 158.36, 163.11. **7b**, **8a**, **8b**, **9a**, and **9b** were also prepared in the same way in 97, 87, 86, 84, and 91% yield, respectively.

Spectroscopic Data of **7b**. mp 40.9−41.7 °C. IR (KBr, cm^{-1}): 3270 (ν_{N-H}), 1683 (amide I), 1512 (amide II), 1247 (ν_{C-O} ether). ^{1}H NMR ($CDCl_3$, rt, 300 MHz, δ): 0.91−0.97 (m, CH_3, 3H), 0.99−1.02 (m, CH_3, 3H), 1.17−1.34 (m, CH_2, 1H), 1.48−1.63 (m, CH_2, 1H), 1.77−1.91 (m, CH, 1H), 3.66−3.82 (m, CH_2, 2H), 6.81−6.90 (m, H_m to NH, 2H), 6.99−7.05 (m, H_o to NH in trans, 1H), 7.40−7.45 (m, H_o to NH in cis, 1H), 7.73 (s, HCO in cis, 0.5H), 8.29 (d, J = 1.8 Hz, NH in cis, 0.5H), 8.44−8.54 (m, HCO and NH in trans, 1H). ^{13}C NMR ($CDCl_3$, rt, 75 MHz, δ): 11.49, 16.70, 26.30, 34.89, 73.38, 73.46, 115.04, 115.69, 121.72, 122.00, 129.60, 130.00, 156.67, 157.56, 159.31, 163.51.

Spectroscopic Data of **8a**. IR (neat, cm^{-1}): 3300 (ν_{N-H}), 1676 (amide I), 1518 (amide II), 1262 (ν_{C-O} ether). ^{1}H NMR ($CDCl_3$, rt, 500 MHz, δ): 0.97 (t, J = 7.5 Hz, CH_3, 3H), 1.03 (d, J = 6.5 Hz, CH_3, 3H), 1.23−1.40 (m, CH_2, 14H), 1.43−1.51 (m, CH_2, 2H), 1.52−1.58 (m, CH_3 and CH_2, 5H), 1.63−1.70 (m, CH_2, 2H), 1.77−1.92 (m, CH_2 and CH, 3H), 4.00 (t, J = 6.5 Hz, CH_2, 2H), 4.12−4.27 (m, CH_2, 4H), 4.73−4.82 (m, CH, 1H), 6.62 (d, J = 8.5 Hz, H_m to NH, 1H), 6.79−6.88 (m, aromatic, 1H), 7.27 (s, aromatic in cis, 0.4H), 7.31 (d, J = 2.0 Hz, aromatic in trans, 0.6H), 7.71 (s, HCO in cis, 0.4H), 8.39 (s, NH in cis, 0.4H), 8.41 (s, HCO in trans, 0.6H), 8.52 (d, J = 11.0 Hz, NH in trans, 0.6H). ^{13}C NMR ($CDCl_3$, rt, 125 MHz, δ): 19.89, 22.82, 22.92, 24.93, 28.20, 30.12, 36.42, 36.53, 37.58, 39.48, 67.80, 68.37, 107.17, 112.26, 112.48, 114.59, 114.88, 130.10, 130.79, 146.47, 147.51, 149.73, 150.31, 158.93, 163.09.

Spectroscopic Data of **8b**. mp 56.9−58.0 °C. IR (KBr, cm^{-1}): 3299 (ν_{N-H}), 1658 (amide I), 1520 (amide II), 1260 (ν_{C-O} ether). ^{1}H NMR ($CDCl_3$, rt, 300 MHz, δ): 0.91−0.98 (m, CH_3, 6H), 1.00−1.05 (m, CH_3, 6H), 1.19−1.36 (m, CH_2, 2H), 1.51−1.66 (m, CH_2, 2H), 1.78−1.96 (m, CH, 2H), 3.70−3.85 (m, CH_2, 4H), 6.59−6.63 (m, H_m to NH, 1H), 6.79−6.90 (m, aromatic, 1.5H), 7.28 (d, J = 2.4 Hz, aromatic, 0.5H), 7.39 (s, HCO in cis, 0.5H), 8.10 (d, J = 11.4 Hz, NH in trans, 0.5H), 8.30 (d, J = 2.1 Hz, NH in cis, 0.5H), 8.52 (d, J = 11.4 Hz, NH in trans, 0.5H). ^{13}C NMR ($CDCl_3$, rt, 75 MHz, δ): 11.55, 16.75, 26.36, 35.05, 35.10, 74.18, 74.36, 74.85, 74.93, 107.08, 107.29, 112.28, 112.36, 114.78, 115.03, 130.18, 130.84, 146.72, 147.75, 150.00, 150.58, 159.06, 163.32.

Spectroscopic Data of **9a**. IR (neat, cm^{-1}): 3303 (ν_{N-H}), 1694 (amide I), 1505 (amide II), 1232 (ν_{C-O} ether). ^{1}H NMR ($CDCl_3$, rt, 500 MHz, δ): 0.87 (d, J = 6.50 Hz, CH_3, 18H), 0.93 (d, J = 6.5 Hz, CH_3, 9H), 1.11−1.37 (m, CH_2, 18H), 1.48−1.63 (m, CH_2, 6H), 1.65−1.74 (m, CH, 3H), 1.78−1.90 (m, CH, 3H), 3.89−4.03 (m, CH_2, 6H), 6.27 (s, H_o to NH in trans, 1H), 6.80 (s, H_o to NH in cis, 1H), 7.14 (s, HCO in cis, 0.5H), 7.68−7.84 (br, HCO in trans, 0.5H), 8.32 (s, NH in cis, 0.5H), 8.58 (d, J = 11.5 Hz, NH in trans, 0.5H). ^{13}C NMR ($CDCl_3$, rt, 125 MHz, δ): 19.79, 22.82, 22.93, 24.95, 28.21, 29.93, 30.03, 36.54, 36.59, 37.56, 37.74, 39.50, 39.60, 67.69, 67.86, 72.00, 72.07, 98.97, 99.25, 107.66, 132.22, 132.67, 135.48, 136.32, 153.49, 154.12, 158.89, 162.72.

Spectroscopic Data of **9b**. mp 42.6−43.4 °C. IR (KBr, cm^{-1}): 3292 (ν_{N-H}), 1678 (amide I), 1508 (amide II), 1230 (ν_{C-O} ether). ^{1}H NMR ($CDCl_3$, rt, 300 MHz, δ): 0.91−0.97 (m, CH_3, 9H), 1.00−1.05 (m, CH_3, 9H), 1.19−1.36 (m, CH_2, 3H), 1.51−1.68 (m, CH_2, 3H), 1.76−1.94 (m, CH, 3H), 3.67−3.83 (m, CH_2, 6H), 6.25 (s, H_o to NH in trans, 1H), 6.78 (s, H_o to NH in cis, 1H), 7.18 (s, HCO in cis, 0.5H), 7.88 (d, J = 11.4 Hz, HCO in trans, 0.5H), 8.30 (d, J = 1.8 Hz, NH in cis, 0.5H), 8.57 (d, J = 11.4 Hz, NH in trans, 0.5H). ^{13}C NMR ($CDCl_3$, rt, 75 MHz, δ): 11.55, 11.65, 16.80, 16.87, 26.33, 26.34, 26.38, 35.12, 35.97, 74.02, 74.18, 78.49, 78.56, 98.63, 98.96, 132.20, 132.64, 135.35, 136.20, 153.62, 154.26, 158.99, 162.95.

Typical Procedure for Syntheses of 1−3. Triethylamine (0.301 mL, 2.16 mmol) was added to a solution of **7a** (300 mg, 1.08 mmol) in dry CH_2Cl_2 (10 mL). After the reaction mixture was stirred at 0 °C for 10 min under Ar, a solution of triphosgene (176 mg, 0.594 mmol) in CH_2Cl_2 (5 mL) was added dropwise to the mixture by the use of a syringe. The dispersion solution was stirred at room temperature for 1 h; then, CH_2Cl_2 (50 mL) was added. After filtration, the solution was washed with aqueous $NaHCO_3$ (100 mL) and dried over anhydrous $MgSO_4$. The solvent was removed under reduced pressure, and the crude product was purified by silica gel chromatography with $CHCl_3$ as the eluent to produce **1a** as a yellow oil (228 mg, 81%). IR (neat, cm^{-1}): 2121 ($\nu_{C\equiv N}$), 1253 (ν_{C-O} ether). ^{1}H NMR ($CDCl_3$, rt, 500 MHz, δ): 0.87 (d, J = 6.5 Hz, CH_3, 6H), 0.93 (d, J = 7.0 Hz, CH_3, 3H), 1.10−1.38 (m, CH_2, 6H), 1.45−1.58 (m, CH_2, 2H), 1.60−1.69 (m, CH, 1H), 1.74−1.83 (m, CH, 1H), 3.91−3.99 (m, CH_2, 2H), 6.82 (d, J = 8.5 Hz, aromatic, 2H), 7.23 (d, J = 8.5 Hz, aromatic, 2H). ^{13}C NMR ($CDCl_3$, rt, 125 MHz, δ): 19.84, 22.82, 22.92, 24.86, 28.18, 30.02, 36.20, 37.46, 39.44, 66.99, 115.28, 119.45, 127.92, 159.70, 162.82. Anal. Calcd for $C_{17}H_{25}NO$ (259.4): C, 78.72; H, 9.71; N, 5.40. Found: C, 78.54; H, 9.80; N, 5.18. $[\alpha]_D^{25}$ − 7.5 (c 0.3, $CHCl_3$). **1b**, **2a**, **2b**, **3a**, and **3b** were also prepared in the same way in 86, 76, 93, 80, and 90% yield, respectively.

Spectroscopic Data of **1b**. IR (neat, cm^{-1}): 2122 ($\nu_{C\equiv N}$), 1256 (ν_{C-O} ether). ^{1}H NMR ($CDCl_3$, rt, 300 MHz, δ): 0.94 (t, J = 7.5 Hz, CH_3, 3H), 1.01 (d, J = 6.6 Hz, CH_3, 3H), 1.19−1.34 (m, CH_2, 1H), 1.48−1.62 (m, CH_2, 1H), 1.78−1.93 (m, CH, 1H), 3.69−3.83 (m, CH_2, 2H), 6.82−6.87 (m, aromatic, 2H), 7.24−7.30 (m, aromatic, 2H). ^{13}C NMR ($CDCl_3$, rt, 75 MHz, δ): 11.40, 16.56, 26.16, 34.72, 73.32, 115.17, 127.78, 159.76, 162.67. Anal. Calcd for $C_{12}H_{15}NO$ (189.3): C, 76.16; H, 7.99; N, 7.40. Found: C, 76.10; H, 8.10; N, 7.24. $[\alpha]_D^{25}$ + 5.7 (c 0.1, $CHCl_3$).

Spectroscopic Data of **2a**. IR (neat, cm^{-1}): 2121 ($\nu_{C\equiv N}$), 1265 (ν_{C-O} ether). ^{1}H NMR ($CDCl_3$, rt, 500 MHz, δ): 0.85 (d, J = 6.5 Hz, CH_3, 12H), 0.94 (d, J = 7.0 Hz, CH_3, 6H), 1.10−1.36 (m, CH_2, 12H), 1.45−1.61 (m, CH_2, 4H), 1.63−1.71 (m, CH, 2H), 1.77−1.86 (m, CH, 2H), 3.93−4.02 (m, CH_2, 4H), 6.76 (d, J = 8.0 Hz, aromatic, 1H), 6.82 (s, aromatic, 1H), 6.88 (d, J = 9.0 Hz, aromatic, 1H). ^{13}C NMR ($CDCl_3$, rt, 125 MHz, δ): 19.88, 22.82, 22.91, 24.92, 28.19, 30.12, 36.19, 36.22, 37.51, 39.44, 67.91, 67.98, 111.60, 113.03, 119.35, 119.51, 149.44, 150.20, 162.46. Anal. Calcd for $C_{27}H_{45}NO_2$ (415.7): C, 78.02; H, 10.91; N, 3.37. Found: C, 78.10; H, 11.05; N, 3.28. $[\alpha]_D^{25}$ − 10.2 (c 0.3, $CHCl_3$).

Spectroscopic Data of **2b**. IR (neat, cm^{-1}): 2122 ($\nu_{C\equiv N}$), 1265 (ν_{C-O} ether). ^{1}H NMR ($CDCl_3$, rt, 300 MHz, δ): 0.92−0.98 (m, CH_3, 6H), 1.01−1.05 (m, CH_3, 6H), 1.21−1.37 (m, CH_2, 2H), 1.50−1.65 (m, CH_2, 2H), 1.82−1.98 (m, CH, 2H), 3.71−3.86 (m, CH_2, 4H), 6.78 (d, J = 8.7 Hz, aromatic, 1H), 6.85 (d, J = 2.4 Hz, aromatic, 1H), 6.91 (d, J = 2.4 Hz, aromatic, 0.5H), 6.93 (d, J = 2.4 Hz, aromatic, 0.5H). ^{13}C NMR ($CDCl_3$, rt, 75 MHz, δ): 11.53,

Table 1. Polymerization Results of 1, 2, and 3 with $NiCl_2 \cdot 6H_2O$ and μ-Ethynediyl Pd−Pt Complex[a]

				polymer						
					yield (%)					
monomer	catalyst	solvent	temp		MeOH-insoluble part	$CHCl_3$-soluble part	$M_n \times 10^{-3b}$	$M_w/M_n{}^b$	$[\alpha]_D^{25c}$	$\Delta\varepsilon_{first}{}^c$
1a	$NiCl_2 \cdot 6H_2O$	CH_2Cl_2	rt	poly-**1a**	49	49	6.7	1.27	+26.5	[d]
1b	$NiCl_2 \cdot 6H_2O$	CH_2Cl_2	rt	poly-**1b**	62	38	2.6[e]	1.22[e]	−12.6[e]	[d,e]
2a	$NiCl_2 \cdot 6H_2O$	CH_2Cl_2	rt	poly-**2a**	67	67	24.0	1.73	+35.5	[d]
2b	$NiCl_2 \cdot 6H_2O$	CH_2Cl_2	rt	poly-**2b**	65	30	8.5[e]	1.80[e]	−186[e]	−4.15[e]
3a	$NiCl_2 \cdot 6H_2O$	CH_2Cl_2	rt	poly-**3a**	61	61	11.0	1.21	+544	+11.5
3b	$NiCl_2 \cdot 6H_2O$	CH_2Cl_2	rt	poly-**3b**	73	41	3.7[e]	1.20[e]	−412[e]	−8.77[e]
3a	Pd−Pt[f]	THF	55 °C	poly-**3a′**	54	54	10.1	1.04	+734	+12.1
3b	Pd−Pt[f]	THF	55 °C	poly-**3b′**	64	35	5.8[e]	1.04[e]	−698[e]	−12.3[e]

[a] Polymerized under N_2; [**1**−**3**] = 0.1 M; [**1**−**3**]/[catalyst] = 100. [b] Determined by SEC (polystyrene standards) with THF containing TBAB (0.1 wt %) as the eluent. [c] Measured in $CHCl_3$ at 25 °C. [d] Not detected. [e] $CHCl_3$-soluble part. [f] μ-Ethynediyl palladium−platinum complex.

16.70, 26.30, 34.91, 34.94, 74.17, 74.22, 111.57, 113.00, 149.64, 150.45, 162.19. Anal. Calcd for $C_{17}H_{25}NO_2$ (275.4): C, 74.14; H, 9.15; N, 5.09. Found: C, 74.01; H, 9.15; N, 5.02. $[\alpha]_D^{25}$ + 16.9 (*c* 0.1, $CHCl_3$).

Spectroscopic Data of **3a**. IR (neat, cm^{-1}): 2121 ($\nu_{C\equiv N}$), 1273 (ν_{C-O} ether). ^1H NMR ($CDCl_3$, rt, 500 MHz, δ): 0.87 (d, J = 7.0 Hz, CH_3, 18H), 0.94 (d, J = 7.0 Hz, CH_3, 9H), 1.08−1.37 (m, CH_2, 18H), 1.47−1.60 (m, CH_2, 6H), 1.65−1.74 (m, CH, 3H), 1.77−1.88 (m, CH, 3H), 3.90−4.01 (m, CH_2, 6H), 6.54 (s, aromatic, 2H). ^{13}C NMR ($CDCl_3$, rt, 125 MHz, δ): 19.76, 22.82, 22.92, 24.93, 28.20, 30.01, 36.36, 36.60, 37.60, 39.46, 67.63, 67.87, 105.27, 121.73, 139.44, 153.51, 162.71. Anal. Calcd for $C_{37}H_{65}NO_3$ (571.9): C, 77.70; H, 11.46; N, 2.45. Found: C, 77.61; H, 11.69; N, 2.20. $[\alpha]_D^{25}$ − 9.7 (*c* 0.3, $CHCl_3$).

Spectroscopic Data of **3b**. IR (neat, cm^{-1}): 2123 ($\nu_{C\equiv N}$), 1228 (ν_{C-O} ether). ^1H NMR ($CDCl_3$, rt, 300 MHz, δ): 0.91−0.97 (m, CH_3, 9H), 1.02−1.05 (m, CH_3, 9H), 1.19−1.36 (m, CH_2, 3H), 1.51−1.67 (m, CH_2, 3H), 1.76−1.96 (m, CH, 3H), 3.68−3.85 (m, CH_2, 6H), 6.56 (s, aromatic, 2H). ^{13}C NMR ($CDCl_3$, rt, 75 MHz, δ): 11.49, 11.61, 16.73, 16.77, 26.25, 34.96, 35.95, 74.12, 78.46, 121.65, 139.33, 153.59, 162.66. Anal. Calcd for $C_{22}H_{35}NO_3$ (361.5): C, 73.09; H, 9.76; N, 3.87. Found: C, 72.84; H, 9.82; N, 3.63. $[\alpha]_D^{25}$ + 7.4 (*c* 0.1, $CHCl_3$).

Polymerization with $NiCl_2 \cdot 6H_2O$. Polymerization was carried out in a dry glass ampule under a dry N_2 atmosphere in a way similar to that previously reported.[8,14] A typical polymerization procedure using $NiCl_2 \cdot 6H_2O$ as the catalyst is described below. Monomer **1a** (20 mg, 0.077 mmol) was placed in a dry ampule, which was then evacuated on a vacuum line and flushed with dry N_2. After this evacuation−flush procedure was repeated three times, a three-way stopcock was attached to the ampule, and dry CH_2Cl_2 (0.77 mL) was added with a syringe. To this was added a solution of $NiCl_2 \cdot 6H_2O$ in dry methanol (0.1 M, 7.7 μL) at room temperature. The concentrations of the monomer and the Ni catalyst were 0.1 and 0.001 M, respectively. The mixture was then stirred under a dry N_2 atmosphere at room temperature. After 1 day, the resulting polymer was precipitated in a large amount of methanol, collected by centrifugation, and then dried in vacuo at room temperature for 2 h to produce poly-**1a** (9.8 mg, 49%). IR (KBr, cm^{-1}): 1672 ($\nu_{C=N}$), 1244 (ν_{C-O} ether). ^1H NMR ($CDCl_3$, 55 °C, 500 MHz, δ): 0.8−1.0 (broad, CH_3, 9H), 1.0−2.0 (broad, CH_2 and CH, 10H), 3.0−4.2 (broad, CH_2, 2H), 5.5−7.7 (broad, aromatic, 4H). Anal. Calcd for $(C_{17}H_{25}NO)_n$: C, 78.72; H, 9.71; N, 5.40. Found: C, 78.44; H, 9.49; N, 5.31. $[\alpha]_D^{25}$ + 26.5 (*c* 0.1, $CHCl_3$). We note that the Ni(II)-catalyzed polymerization in the presence of air[15] produced a lower-molecular-weight polymer, and therefore, the polymerization was performed in the absence of air. In the same way, poly-**1b**, poly-**2a**, poly-**2b**, poly-**3a**, and poly-**3b** were prepared in 62, 67, 65, 61, and 73% yield, respectively. Parts of poly-**1b**, poly-**2b**, and poly-**3b** were insoluble in common organic solvents, and $CHCl_3$-soluble parts were collected by extraction with $CHCl_3$ and were used for further spectroscopic measurements. (See Table 1.)

*Spectroscopic Data of Poly-***1b**. IR (KBr, cm^{-1}): 1668 ($\nu_{C=N}$), 1245 (ν_{C-O} ether). ^1H NMR ($CDCl_3$, 55 °C, 500 MHz, δ): 0.8−1.2 (broad, CH_3, 6H), 1.2−2.0 (broad, CH_2 and CH, 3H), 2.8−4.0 (broad, CH_2, 2H), 5.5−7.6 (broad, aromatic, 4H). Anal. Calcd for $(C_{12}H_{15}NO \cdot 3/7H_2O)_n$: C, 73.17; H, 8.11; N, 7.11. Found: C, 73.02; H, 8.35; N, 6.90. $[\alpha]_D^{25}$ − 12.6 (*c* 0.1, $CHCl_3$).

*Spectroscopic Data of Poly-***2a**. IR (KBr, cm^{-1}): 1634 ($\nu_{C=N}$), 1221 (ν_{C-O} ether). ^1H NMR ($CDCl_3$, 55 °C, 500 MHz, δ): 0.8−1.0 (broad, CH_3, 18H), 1.0−2.0 (broad, CH_2 and CH, 20H), 2.7−4.3 (broad, CH_2, 4H), 4.8−7.1 (broad, aromatic, 3H). Anal. Calcd for $(C_{27}H_{45}NO_2)_n$: C, 78.02; H, 10.91; N, 3.37. Found: C, 77.95; H, 10.84; N, 3.37. $[\alpha]_D^{25}$ + 35.5 (*c* 0.1, $CHCl_3$).

*Spectroscopic Data of Poly-***2b**. IR (KBr, cm^{-1}): 1651 ($\nu_{C=N}$), 1222 (ν_{C-O} ether). ^1H NMR ($CDCl_3$, 55 °C, 500 MHz, δ): 0.8−1.2 (broad, CH_3, 12H), 1.2−2.1 (broad, CH_2 and CH, 6H), 2.8−4.1 (broad, CH_2, 4H), 5.0−7.3 (broad, aromatic, 3H). Anal. Calcd for $(C_{17}H_{25}NO_2 \cdot {}^1/_2H_2O)_n$: C, 71.80; H, 9.21; N, 4.93. Found: C, 71.82; H, 9.45; N, 4.83. $[\alpha]_D^{25}$ − 186 (*c* 0.1, $CHCl_3$).

*Spectroscopic Data of Poly-***3a**. IR (KBr, cm^{-1}): 1645 ($\nu_{C=N}$), 1225 (ν_{C-O} ether). ^1H NMR ($CDCl_3$, 55 °C, 500 MHz, δ): 0.8−1.0 (broad, CH_3, 27H), 1.0−2.0 (broad, CH_2 and CH, 30H), 2.9−4.8 (broad, CH_2, 6H), 5.1−6.1 (broad, aromatic, 2H). Anal. Calcd for $(C_{37}H_{65}NO_3)_n$: C, 77.70; H, 11.46; N, 2.45. Found: C, 77.59; H, 11.50; N, 2.30. $[\alpha]_D^{25}$ + 544 (*c* 0.1, $CHCl_3$).

*Spectroscopic Data of Poly-***3b**. IR (KBr, cm^{-1}): 1651 ($\nu_{C=N}$), 1223 (ν_{C-O} ether). ^1H NMR ($CDCl_3$, 55 °C, 500 MHz, δ): 0.8−1.1 (broad, CH_3, 18H), 1.1−2.1 (broad, CH_2 and CH, 9H), 2.7−4.2 (broad, CH_2, 6H), 5.0−6.2 (broad, aromatic, 2H). Anal. Calcd for $(C_{22}H_{35}NO_3)_n$: C, 73.09; H, 9.76; N, 3.87. Found: C, 73.02; H, 9.68; N, 3.81. $[\alpha]_D^{25}$ − 412 (*c* 0.1, $CHCl_3$).

Polymerization with Pd−Pt Complex. Polymerization with the μ-ethynediyl Pd−Pt complex as the catalyst was carried out in dry THF under a dry N_2 atmosphere in a way similar to that previously reported.[13] A typical polymerization procedure is described below. Monomer **3a** (100 mg, 0.17 mmol) was placed in a dry ampule, which was then evacuated on a vacuum line and flushed with dry N_2. After this evacuation−flush procedure was repeated three times, a three-way stopcock was attached to the ampule, and dry THF (1.01 mL) was added with a syringe. To this was added a solution of the μ-ethynediyl Pd−Pt complex in dry THF (2.4 mM, 0.74 mL) at room temperature. The concentrations of the monomer and the catalyst were 0.1 and 0.001 M, respectively. The mixture was then stirred under a dry N_2 atmosphere and heated to 55 °C. After 20 h, the resulting polymer was precipitated in a large amount of methanol, collected by centrifugation, and then dried in vacuo at room temperature overnight to produce poly-**3a′** (53.6 mg, 54%). IR (KBr, cm^{-1}): 1644 ($\nu_{C=N}$), 1224 (ν_{C-O} ether). ^1H NMR ($CDCl_3$, 55 °C, 500 MHz, δ): 0.85 (broad, CH_3, 27H), 1.0−2.0 (broad, CH_2 and CH, 30H), 3.0−4.3 (broad, CH_2, 6H), 5.0−6.2 (broad, aromatic, 2H). Anal. Calcd for $(C_{37}H_{65}NO_3)_n$: C, 77.70; H, 11.46; N, 2.45. Found: C, 77.69; H, 11.57; N, 2.48. $[\alpha]_D^{25}$ + 734 (*c* 0.1, $CHCl_3$). In the same way, poly-**3b′** was prepared in 64% yield. A part of poly-**3b′** was insoluble in common organic solvents, and a $CHCl_3$-soluble part was collected by extraction with $CHCl_3$ and used for further spectroscopic measurements. (See Table 1.)

*Spectroscopic Data of Poly-***3b′**. IR (KBr, cm^{-1}): 1651 ($\nu_{C=N}$), 1225 (ν_{C-O} ether). ^1H NMR ($CDCl_3$, 55 °C, 500 MHz, δ): 0.8−1.4 (broad, CH_3, 18H), 1.4−2.1 (broad, CH_2 and CH, 9H), 2.9−3.9

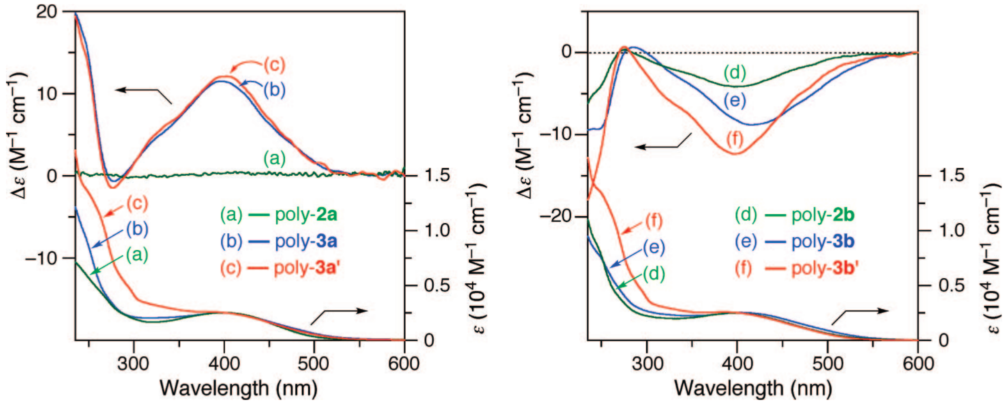

Figure 1. CD and absorption spectra of (a) poly-**2a**, (b) poly-**3a**, (c) poly-**3a′**, (d) poly-**2b**, (e) poly-**3b**, and (f) poly-**3b′** (0.2 mg/mL) in $CHCl_3$ at 25 °C.

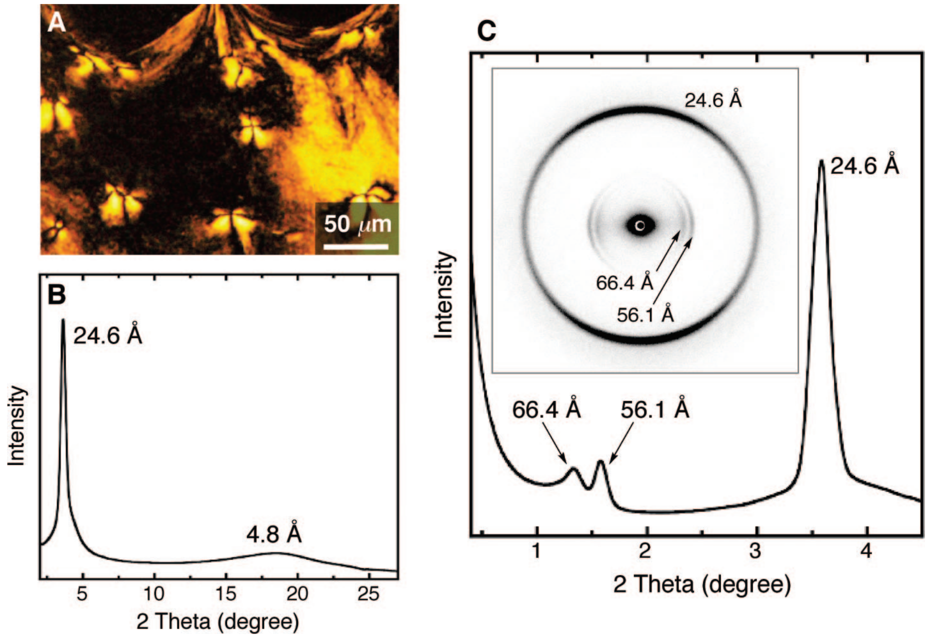

Figure 2. (A) Polarized optical micrograph of poly-**3a** measured at 200 °C upon heating and (B) WAXD pattern of poly-**3a** measured at 200 °C. (C) SAXS profiles of poly-**3a** measured at 200 °C. Inset shows a SAXS pattern of poly-**3a** measured at 200 °C.

(broad, CH_2, 6H), 5.3−6.4 (broad, aromatic, 2H). Anal. Calcd for $(C_{22}H_{35}NO_3)_n$: C, 73.09; H, 9.76; N, 3.87. Found: C, 72.99; H, 9.88; N, 3.86. $[\alpha]_D^{25}$ − 698 (*c* 0.1, $CHCl_3$).

Molecular Modeling and Calculations. The molecular modeling and molecular mechanics (MM) calculations were conducted with the Compass force field,[16] as contained in the MS Modeling software (version 4.0, Accelrys, San Diego, CA) operated using a PC running under Windows XP. The polymer models (50 repeating monomer units) of poly-**1a**−poly-**3a** and poly-**3b** were constructed using the Polymer Builder module in the MS Modeling software with the suitable side-chain conformations. The starting main-chain geometrical parameters, such as the bond lengths, the bond angles, and the internal rotation angles were defined as a 15 unit/4 turn (15/4) helix with either a right- or a left-handed helical structure on the basis of the right- and left-handed helical structures of the poly(phenyl isocyanide)s bearing L-alanine pendants with an *n*-decyl chain determined by X-ray analysis.[13] The geometric parameters of the main chain were fixed during the following force-field optimization. The dielectric constant was set to 1.0. The geometry optimizations were carried out without any cutoff by the smart minimizer in three steps. First, the starting conformations were subject to the steepest decent optimization to eliminate the worse steric conflicts. Second, subsequent optimization until the convergence using a conjugate gradient algorithm was performed. The fully optimized polymer models were obtained by the further energy minimization using the Newton method with the 0.1 kcal/mol/Å convergence criterion; the bond lengths, the bond angles, and the internal rotation angles of the main chains were 68.4°, 108.0°, and 1.42 Å for right-handed helical poly-**1a**−poly-**3a** and −67.1°, 106.8°, and 1.46 Å for left-handed helical poly-**3b**, respectively (Figure 3).[13]

Results and Discussion

Six new optically active phenyl isocyanide monomers (**1a**−**3a** and **1b**−**3b**) were prepared according to Schemes 1 and 2 without any difficulty. All monomers were purified by column chromatography and then characterized and identified by the use of ^{1}H and ^{13}C NMR spectroscopies and elemental analyses. These monomers were then polymerized with an achiral $NiCl_2$ in CH_2Cl_2 at room temperature (Scheme 1) or with the Pd−Pt complex[10b,13] (**3a** and **3b**) in THF at 55 °C (Scheme 2). The polymerization reactions of **1a**−**3a** homogeneously proceeded and afforded relatively high molecular weight polymers ($M_n = 6.7 \times 10^3$ to 2.4×10^4 for poly-**1a**−poly-**3a** and poly-**3a′**) in moderate yield (49−67%), whereas the polymers partially precipitated during the polymerization of

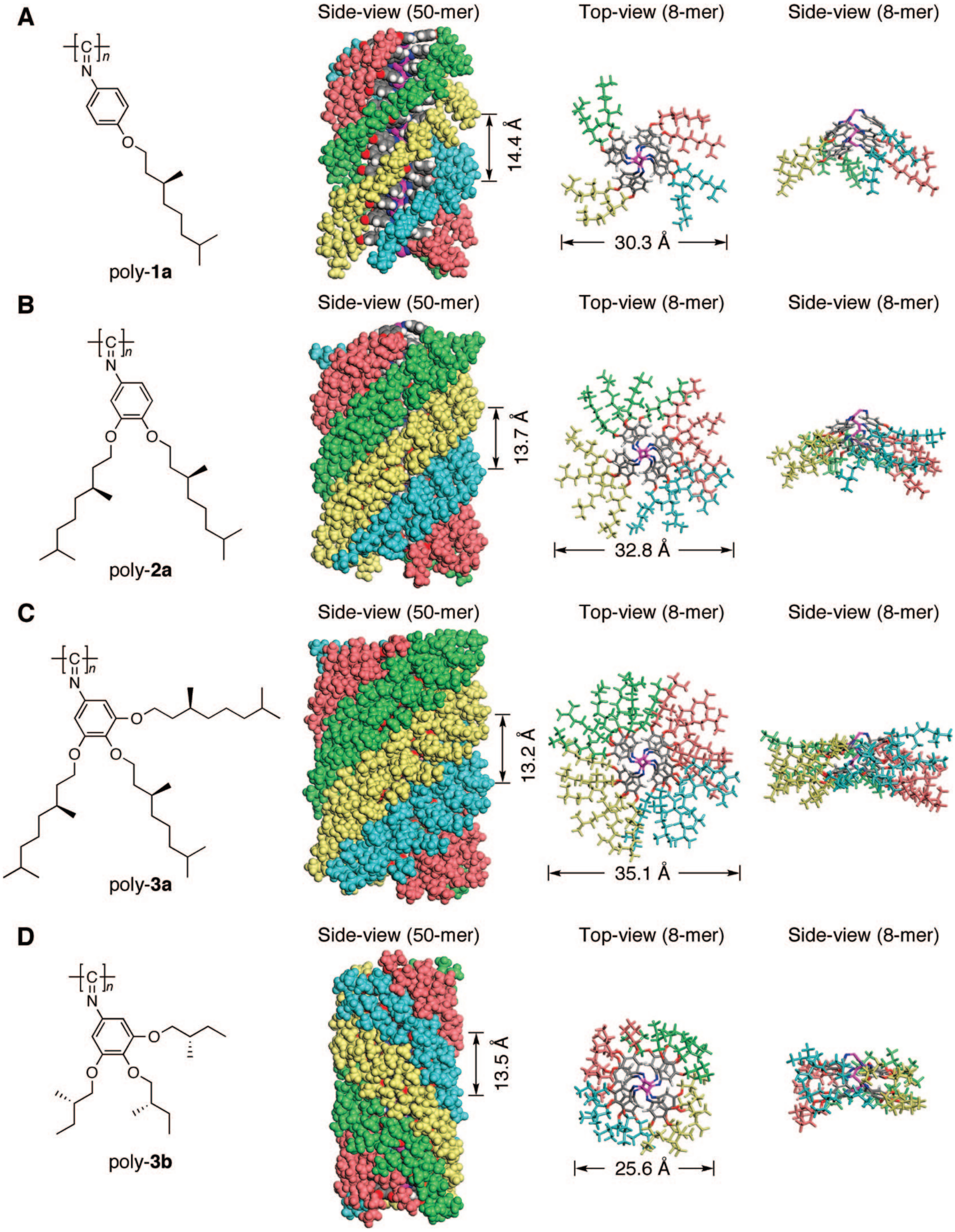

Figure 3. Possible helical structures of (A) right-handed helical poly-**1a**, (B) right-handed helical poly-**2a**, (C) right-handed helical poly-**3a**, and (D) left-handed helical poly-**3b** on the basis of X-ray structural analyses followed by molecular mechanics calculation. Each structure is represented by space-filling (50-mer, left) and ball-and-stick models (8-mer, right). Four sets of helical arrays (*n* and *n* + 4) of the pendants are shown in different colors for clarity (orange, green, yellow, and light blue).

1b−**3b**, and the molecular weights of the CHCl$_3$-soluble fractions of poly-**1b**−poly-**3b** and poly-**3b′** were rather low ($M_n = 2.6-8.5 \times 10^3$). (See the Experimental Section and Table 1).

We first investigated the steric and odd−even effects of the chiral pendants on the chiroptical properties of the resulting polyisocyanides using CD spectroscopy. Poly-**1a**, poly-**2a**, and poly-**1b** showed no detectable CD in CHCl$_3$ at 25 °C. However, poly-**3a** and poly-**3a′** bearing tri-(*S*)-3,7-dimethyloctyloxyphenyl pendants and poly-**2b,** poly-**3b**, and poly-**3b′** having di- or tri-(*S*)-2-methylbutoxyphenyl pendants whose stereogenic centers are located close to the polymer backbones showed apparent CDs with the first Cotton effects in the imino chromophore regions of the polymer backbones at ~400 nm ($\Delta\varepsilon_{\text{first}}$) (Figure 1), although poly-**2b** exhibited a relatively weak CD compared with those of the polyisocyanides bearing trialkoxy pendants. The $\Delta\varepsilon_{\text{first}}$ value tended to increase with an increase in the number of alkoxy chains (poly-**2** < poly-**3**), and the polyisocyanides bearing fan-shaped, bulky trialkoxy chains (poly-**3**) showed intense Cotton effects because of large steric hindrance between the neighboring chiral chains of the pendants. The effect of the molecular weights of the polyisocyanides on the CD intensity may be negligibly small because the low-molecular-weight poly-**2b** ($M_n = 8.5 \times 10^3$) and poly-**3b** ($M_n = 3.7 \times 10^3$) showed

Table 2. WAXD Results of Polyisocyanides[a]

polymer	lateral spacing (Å)	spacing between alkoxybenzene units (Å)
poly-**1a**	23.7	4.7
poly-**1b**	18.1	4.7
poly-**2a**	24.1	4.7
poly-**2b**	18.4	4.6
poly-**3a**	24.3	4.7
poly-**3b**	18.6	4.6
poly-**3a′**	23.9	4.7
poly-**3b′**	18.4	4.6

[a] WAXD measurements were performed at ambient temperature.

apparent Cotton effects, whereas the high-molecular-weight poly-**2a** exhibited no CD ($M_n = 2.4 \times 10^4$) (Table 1).

The position of the stereogenic center (odd−even effect) biased the helical sense of the polyisocyanides, thus showing the positive (poly-**3a** and poly-**3a′**) and opposite negative (poly-**2b**, poly-**3b**, and poly-**3b′**) first Cotton effects. In addition, the fact that poly-**3a** exhibited a more intense Cotton effect than that of poly-**3b** indicates that the steric effect rather than the position of the stereogenic center plays an important role in the preferred-handed helicity induction in the fan-shaped, bulky poly-**3**. On the basis of the first Cotton effect sign, the former polyisocyanides were assigned to have a right-handed helix, and the latter were assigned to have an opposite left-handed helix.[13,17] The appearance of the CD in poly-**2b** suggests that the long-range preferred-handed helicity induction in the poly-**2b** main-chain induced by the chiral pendant groups with a stereogenic center located closely to the phenyl groups is superior to that in poly-**2a**.[4a−c,e,18] The specific rotation ($[\alpha]_D^{25}$) values of the polyisocyanides also support the above arguments (Table 1); the CD-active polyisocyanides showed relatively large specific rotations (−186 to −698° and +544 to +734°) and the polyisocyanides with the opposite $\Delta\varepsilon_{\text{first}}$ value also had the opposite specific rotation signs.

We then investigated the lyotropic liquid crystallinity of the polyisocyanides in various solvents, but all of the polyisocyanides showed no lyotropic LC phase. However, variable-temperature POM observations revealed that poly-**3a** showed a thermotropic LC phase at ∼150 °C upon heating, but no further phase transition was observed before the decomposition at 250 °C. Figure 2A shows a polarized optical micrograph of poly-**3a** at 200 °C. A clear birefringence was observed, but we could not identify the phase.[6,11] In addition, this LC texture was retained after slow cooling to room temperature. No birefringence due to thermotropic LC formations was observed for the other polyisocyanides upon heating; the reason for this is not presently clear.

Variable-temperature XRD measurements of poly-**3a** were then performed to gain information on the mesomorphic structure. Figure 2B,C shows the WAXD and SAXS patterns of poly-**3a** measured at 200 °C, respectively. The WAXD diagram showed sharp and broad peaks at 3.59 and ca. 18.5°, respectively (Figure 2B), suggesting a lateral spacing of 24.6 Å due to the lateral packing of the polymer molecules and a periodic reflection of 4.8 Å corresponding to a spacing between the alkoxybenzene units, respectively. Similar WAXD patterns were observed for dendronized helical polyacetylenes[6,7] and polyisocyanides.[11] The SAXS pattern showed two more weak peaks in the small-angle regions ($2\theta = 1.33$ and 1.58°, Figure 2C). These results revealed that poly-**3a** forms a highly ordered assembled structure in which several mesogenic polymer chains were associated in a layer, column, or lattice in the temperature range between 150 and 250 °C.[6,11,19] However, the detailed assembled structure of poly-**3a** remains unclear because the two peaks observed in the SAXS corresponding to 66.4 and 56.1 Å could not be identified.

The WAXD measurement results of other polyisocyanides including poly-**3a** are summarized in Table 2. The lateral spacing slightly increased with the increasing number of alkoxy chains, but the difference is not significant. The fact that all polyisocyanides showed a similar reflection due to the neighboring alkoxybenzene units (4.6 to 4.7 Å) suggests that the polymers may possess a similar helical structure, although poly-**1a**, poly-**2a**, and poly-**1b** exist as an equal mixture of the right- and left-handed helices and thus show no CD. Figure 3A−C shows possible helical structures of the right-handed helical poly-**1a**, poly-**2a**, and poly-**3a**, respectively, and the left-handed helical poly-**3b** (D) on the basis of a 15/4 helical structure of right- and left-handed helical polyisocyanides bearing L-alanine pendants with a long *n*-decyl chain determined by X-ray structural analyses, followed by MM calculations.[13] (See the Experimental Section.) The diameters of the calculated cylindrical polyisocyanides also slightly increased with an increase in the number of alkoxy chains. The calculated diameters of the polyisocyanides were, however, significantly larger than the lateral spacing values observed by the WAXD measurements (Table 2), suggesting that the aliphatic pendant groups may overlap in an interdigitated manner.[6]

In summary, we synthesized a series of optically active polyisocyanides bearing mono-, di-, or tri-(*S*)-alkoxy chains with a stereogenic center at a position different from that of the pendants and found that the steric effects and the position of the stereogenic center played a crucial role in biasing a preferred-handed helicity in the polymer backbones. The polyisocyanides bearing fan-shaped, bulky trialkoxy chains efficiently biased the helical sense of the polyisocyanides and exhibited intense Cotton effects irrespective of the position of the stereogenic center, whereas a clear odd−even effect was observed for the polyisocyanides with di- and trialkoxy chains. The thermotropic LC formation of a helical polyisocyanide with a fan-shaped pendant (poly-**3a**) may provide novel chiral LC materials. Further elucidation of the self-assembled structure of the helical polyisocyanide in the LC state will be the objective of future studies.

Acknowledgment. We are deeply grateful to Professor K. Onitsuka (Osaka University) for his generous supply of the Pd−Pt catalyst. H.L. thanks the Japan Society for the Promotion of Science (JSPS) for a postdoctoral fellowship for foreign researchers (no. P04398). K.N. expresses his thanks for a JSPS Research Fellowship for Young Scientists (no. 6683).

References and Notes

(1) For reviews on helical polymers, see: (a) Okamoto, Y.; Nakano, T. *Chem. Rev.* **1994**, *94*, 349–372. (b) Nolte, R. J. M. *Chem. Soc. Rev.* **1994**, *23*, 11–19. (c) Green, M. M.; Park, J.-W.; Sato, T.; Teramoto, A.; Lifson, S.; Selinger, R. L. B.; Selinger, V. B.; Selinger, J. V. *Angew. Chem., Int. Ed.* **1999**, *38*, 3138–3154. (d) Nakano, T.; Okamoto, Y. *Chem. Rev.* **2001**, *101*, 4013–4038. (e) Cornelissen, J. J. L. M.; Rowan, A. E.; Nolte, R. J. M.; Sommerdijk, N. A. J. M. *Chem. Rev.* **2001**, *101*, 4039–4070. (f) Nomura, R.; Nakako, H.; Masuda, T. *J. Mol. Catal. A: Chem.* **2002**, *190*, 197–205. (g) Fujiki, M.; Koe, J. R.; Terao, K.; Sato, T.; Teramoto, A.; Watanabe, J. *Polym. J.* **2003**, *35*, 297–344. (h) Yashima, E.; Maeda, K.; Nishimura, T. *Chem.−Eur. J.* **2004**, *10*, 43–51. (i) Suginome, M.; Ito, Y. *Adv. Polym. Sci.* **2004**, *17*, 77–136. (j) Lam, J. W. Y.; Tang, B. Z. *Acc. Chem. Res.* **2005**, *38*, 745–754. (k) Aoki, T.; Kaneko, T.; Teraguchi, M. *Polymer* **2006**, *37*, 717–735. (l) Maeda, K.; Yashima, E. *Top. Curr. Chem.* **2006**, *265*, 47–88. (m) Yashima, E.; Maeda, K. *Macromolecules* **2008**, *41*, 3–12. (n) Pijper, D.; Feringa, B. L. *Soft Matter* **2008**, *4*, 1349–1372. (o) Yashima, E.; Maeda, K.; Furusho, Y. *Acc. Chem. Res.* **2008**, *41*, 1166–1180.

(2) For selective references of helix-sense-selective polymerization of achiral monomers with chiral initiators or catalysts, see: (a) Okamoto, Y.; Suzuki, K.; Ohta, K.; Hatada, K.; Yuki, H. *J. Am. Chem. Soc.* **1979**, *101*, 4763–4765. (b) Kamer, P. C. J.; Cleiji, M. C.; Nolte, R. J. M.; Harada, T.; Hezemans, A. M. F.; Drenth, W. *J. Am. Chem. Soc.* **1988**, *110*, 1581–1587. (c) Nakano, T.; Okamoto, Y.; Hatada, K. *J. Am. Chem. Soc.* **1992**, *114*, 1318–1329. (d) Deming, T. J.; Novak, B. M. *J. Am. Chem. Soc.* **1992**, *114*, 7926–7927. (e) Vogl, O.; Jaycox, G. D.; Kratky, C.; Simonsick, W. J.; Hatada, K. *Acc. Chem. Res.* **1992**, *25*, 408–413. (f) Okamoto, Y.; Matsuda, M.; Nakano, T.; Yashima, E. *Polym. J.* **1993**, *25*, 391–396. (g) Aoki, T.; Kaneko, T.; Maruyama, N.; Sumi, A.; Takahashi, M.; Sato, T.; Teraguchi, M. *J. Am. Chem. Soc.* **2003**, *125*, 6346–6347. (h) Tian, G.; Lu, Y.; Novak, B. M. *J. Am. Chem. Soc.* **2004**, *126*, 4082–4083.

(3) For leading references of hydrogen-bond-assisted helical polymers, see ref 2g and: (a) Cornelissen, J. J. L. M.; Fischer, M.; Sommerdijk, N. A. J. M.; Nolte, R. J. M *Science* **1998**, *280*, 1427–1430. (b) Cornelissen, J. J. L. M.; Donners, J. J. J. M.; de Gelder, R.; Graswinckel, W. S.; Metselaar, G. A.; Rowan, A. E.; Sommerdijk, N. A. J. M.; Nolte, R. J. M. *Science* **2001**, *293*, 676–680. (c) Nomura, R.; Tabei, J.; Masuda, T. *J. Am. Chem. Soc.* **2001**, *123*, 8430–8431. (d) Cornelissen, J. J. L. M.; Graswinckel, W. S.; Rowan, A. E.; Sommerdijk, N. A. J. M.; Nolte, R. J. M. *J. Polym. Sci., Part A: Polym. Chem.* **2003**, *41*, 1725–1736. (e) Li, B. S.; Cheuk, K. K. L.; Ling, L.; Chen, J.; Xiao, X.; Bai, C.; Tang, B. Z. *Macromolecules* **2003**, *36*, 77–85. (f) Metselaar, G. A.; Cornelissen, J. J. L. M.; Rowan, A. E.; Nolte, R. J. M. *Angew. Chem., Int. Ed.* **2005**, *44*, 1990–1993. (g) Okoshi, K.; Sakajiri, K.; Kumaki, J.; Yashima, E. *Macromolecules* **2005**, *38*, 4061–4064. (h) Okoshi, K.; Sakurai, S.-i.; Ohsawa, S.; Kumaki, J.; Yashima, E. *Angew. Chem., Int. Ed.* **2006**, *45*, 8173–8176.

(4) (a) Ramos, E.; Bosch, J.; Serrano, J.-L.; Sierra, T.; Veciana, J. *J. Am. Chem. Soc.* **1996**, *118*, 4703–4704. (b) Amabilino, D. B.; Ramos, E.; Serrano, J.-L.; Sierra, T.; Veciana, J. *J. Am. Chem. Soc.* **1998**, *120*, 9126–9134. (c) Amabilino, D. B.; Ramos, E.; Serrano, J.-L.; Veciana, J. *Adv. Mater.* **1998**, *10*, 1001–1005. (d) Gomar-Nadal, E.; Veciana, J.; Rovira, C.; Amabilino, D. B. *Adv. Mater.* **2005**, *17*, 2095–2098. (e) Amabilino, D. B.; Serrano, J.-L.; Sierra, T.; Veciana, J. *J. Polym. Sci. Part A: Polym. Chem.* **2006**, *44*, 3161–3174. For other leading references on helical polyisocyanides except for poly(isocyanopeptide)s,[1e,3a,b,d,f] see: (f) Hasegawa, T.; Kondoh, S.; Matsuura, K.; Kobayashi, K. *Macromolecules* **1999**, *32*, 6595–6603. (g) Yamada, Y.; Kawai, T.; Abe, J.; Iyoda, T. *J. Polym. Sci., Part A: Polym. Chem.* **2002**, *40*, 399–408.

(5) (a) Oda, M.; Nothofer, H.-G.; Scherf, U.; Sunjic, V.; Richter, D.; Regenstein, W.; Neher, D. *Macromolecules* **2002**, *35*, 6792–6798. (b) Yamazaki, K.; Yokoyama, A.; Yokozawa, T. *Macromolecules* **2002**, *35*, 2432–2434. (c) Henze, O.; Feast, W. J.; Gardebien, F.; Jonkheijm, P.; Lazzaroni, R.; Leclere, P.; Meijer, E. W.; Schenning, A. P. H. J. *J. Am. Chem. Soc.* **2006**, *128*, 5923–5929. (d) Zhi, J.; Zhu, Z.; Liu, A.; Cui, J.; Wan, X.; Zhou, Q. *Macromolecules* **2008**, *41*, 1594–1597.

(6) Schenning, A. P. H. J.; Fransen, M.; Meijer, E. W. *Macromol. Rapid Commun.* **2002**, *23*, 265–270.

(7) (a) Percec, V.; Rudick, J. G.; Peterca, M.; Wagner, M.; Obata, M.; Mitchell, C. M.; Cho, W.-D.; Balagurusamy, V. S. K.; Heiney, P. A. *J. Am. Chem. Soc.* **2005**, *127*, 15257–15264. (b) Percec, V.; Aqad, E.; Peterca, M.; Rudick, J. G.; Lemon, L.; Ronda, J. C.; De, B. B.; Heiney, P. A.; Meijer, E. W. *J. Am. Chem. Soc.* **2006**, *128*, 16365–16372. (c) Rudick, J. G.; Percec, V. *New J. Chem.* **2007**, *31*, 1083–1096.

(8) Kajitani, T.; Okoshi, K.; Sakurai, S.-i.; Kumaki, J.; Yashima, E. *J. Am. Chem. Soc.* **2006**, *128*, 708–709.

(9) Kajitani, T.; Okoshi, K.; Yashima, E. *Macromolecules* **2008**, *41*, 1601–1611.

(10) (a) Onitsuka, K.; Joh, T.; Takahashi, S. *Bull. Chem. Soc. Jpn.* **1992**, *65*, 1179–1181. (b) Onitsuka, K.; Joh, T.; Takahashi, S. *Angew. Chem., Int. Ed. Engl.* **1992**, *31*, 851–852. (c) Takei, F.; Yanai, K.; Onitsuka, K.; Takahashi, S. *Angew. Chem., Int. Ed.* **1996**, *35*, 1554–1556. (d) Takei, F.; Yanai, K.; Onitsuka, K.; Takahashi, S. *Chem.—Eur. J.* **2000**, *6*, 983–993. (e) Takei, F.; Hayashi, H.; Onitsuka, K.; Kobayashi, N.; Takahashi, S. *Angew. Chem., Int. Ed.* **2001**, *40*, 4092–4094. (f) Hida, N.; Takei, F.; Onitsuka, K.; Shiga, K.; Asaoka, S.; Iyoda, T.; Takahashi, S. *Angew. Chem., Int. Ed.* **2003**, *42*, 4349–4352.

(11) Recently, polyisocyanides bearing achiral dendronized pendant groups were prepared, and their thermotropic LC properties and the formation of supramolecular nanostructures were reported. See: Tian, Y.; Kamata, K.; Yoshida, H.; Iyoda, T. *Chem.—Eur. J.* **2006**, *12*, 584–591.

(12) Yelamaggad, C. V.; Achalkumar, A. S. *Tetrahedron Lett.* **2006**, *47*, 7071–7075.

(13) Onouchi, H.; Okoshi, K.; Kajitani, T.; Sakurai, S.-i.; Nagai, K.; Kumaki, J.; Onitsuka, K.; Yashima, E. *J. Am. Chem. Soc.* **2008**, *130*, 229–236.

(14) Ishikawa, M.; Maeda, K.; Yashima, E. *J. Am. Chem. Soc.* **2002**, *124*, 7448–7458.

(15) Deming, T. J.; Novak, B. M. *Macromolecules* **1991**, *24*, 5478–5480.

(16) Sun, H. *J. Phys. Chem. B* **1998**, *102*, 7338–7364.

(17) High-resolution AFM observations of the diastereomeric polyisocyanides revealed that the polyisocyanides having a positive $\Delta\varepsilon_{\text{first}}$ value display a right-handed helical structure. See refs 8 and 13.

(18) Onitsuka, K.; Mori, T.; Yamamoto, M.; Takei, F.; Takahashi, S. *Macromolecules* **2006**, *39*, 7224–7231.

(19) Percec, V.; Ann, C. H.; Ungar, G.; Yeardley, D. J. P.; Moller, M.; Sheiko, S. S. *Nature* **1998**, *391*, 161–164.

MA802345G